Operational Process for Manufacturing a MEMS Micro-Cantilever System

KAFUMBE Said[1, a], DANTHAKANI Ravichandran[2, b], ABD-ELRADY Emad[3, c], ALQUDAH Mohammad[4, d]
Department of Electronic Engineering Technology,
Higher Colleges of Technology,
Abu Dhabi, UAE
[a]skafumbe@hct.ac.ae, [b]rdanthakani@hct.ac.ae,
[c]eabdelrady@hct.ac.ae, [d]malqudah@hct.ac.ae,

HARRIS Alun[5, e], BURDESS Jim[6, f]
[e] School of Electrical, Electronics and Computer Engineering, [f] School of Mechanical Systems Engineering,
Newcastle University,
UK
[e]alun.harris@ncl.ac.uk , [f]jim.burdess@ncl.ac.uk

***Abstract*—The processing techniques and materials utilized in the fabrication of a two-terminal electrostatically actuated micro-electro-mechanical (MEMS) cantilever-arrayed device used for radio frequency tuning applications are presented in this work. The process is based on silicon surface micromachining with spin-coated photoresist as the sacrificial layer placed underneath the electroplated gold structural material and an insulating layer of silicon dioxide. Silicon dioxide layer is deposited using plasma enhanced chemical vapour deposition (PECVD), to avoid a short circuit between the cantilever and the bottom electrode. The fabrication process involves six major steps designed under controlled experiments. These includes the plasma enhanced chemical vapour deposition of the silicon dioxide insulating layer, optical lithography to transfer photomask layer patterns, vacuum evaporation to deposit thin films of Titanium (Ti) and Gold (Au), electroplating of Au, the dry release of the cantilever beam arrays, and finally the wafer dicing to split the different micro devices. These process steps were each sub-detailed to give a total of fourteen micro-fabrication processes. Scanning electron microscope (SEM) images taken on the final fabricated device that was dry released using oxygen plasma ashing to avoid stiction, showed twelve freely suspended micro-cantilevered beams suspended with an average electrostatic gap of 2.29±0.17 microns above a 4934±3 angstrom thick silicon dioxide layer. Preliminary dimensional measurements on the fabricated devices revealed that the cantilevers were at least 52.06±1.93 microns wide with lengths varying from 377.97±0.01microns to 1491.89±0.01 microns, and were at least 2.21±0.05 microns thick. These results were validated by design values.**

Keywords— MEMS; Micro-Cantilever; Manufacturing process, Gold electrodeposition

I. INTRODUCTION

Micro-Electro-Mechanical Systems (MEMS) or micromachines are an important innovation in technology that have shown dramatic advances in the semiconductor industry [1]. This technology enables the fabrication of machines that are vanishingly small, very cheap, and have the ability to function in a variety of applications. However, to achieve these attributes, there is always need to optimize the MEMS fabrication process so that it involves less steps, uses fewer lithographic masks, and achieves a high yield. The process presented in this work uses three photo masks in a six step fabrication process, which includes a final dry release step aimed at achieving fully suspended stiction free MEMS-cantilevers thus increasing the yield. A sketch of the suspended MEMS-cantilever is shown in Fig. 1 and fabricated devices in Fig. 2. Micromachining, microfabrication, micromanufacturing and microelectromechanical systems (MEMS) fabrication all relate to processes aimed at developing devices with at least some of their dimensions in the micrometer range, and whose applications extend from

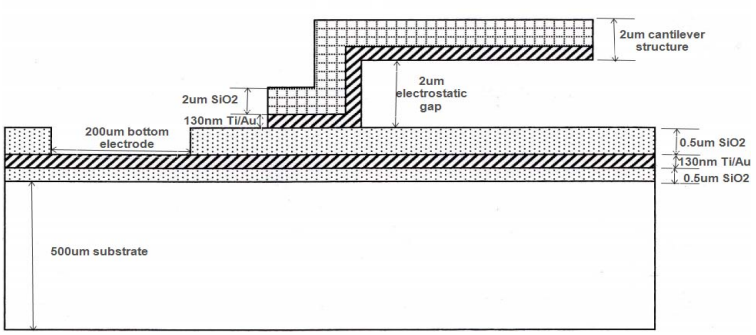

Fig. 1. Sketch of a Suspended MEMS-Cantilever

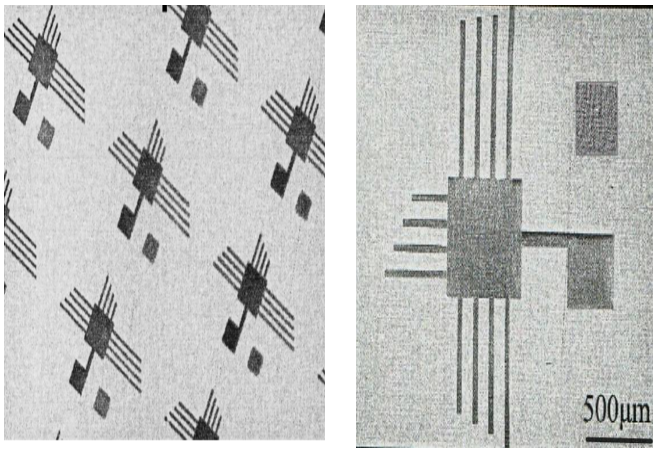

Fig. 2. (a) SEM pictures of many fabricated devices on a single wafer before dicing; (b) Close-up of a diced MEMS-Cantilever device

978-1-4799-6065-1/15/$31.00 ©2015 IEEE

silicon-based mechanical purposes to biotechnology, and information and communication technologies [2]. As a result,

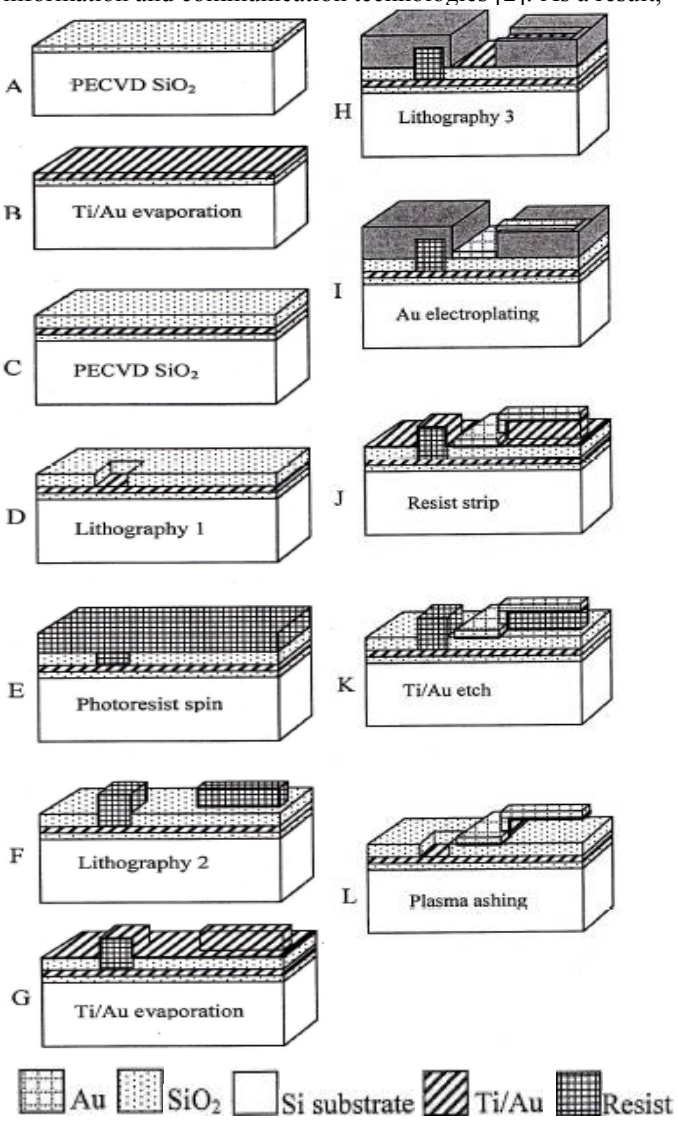

Fig. 3. Simplified fabrication process

MEMS refers to all sub-miniaturised systems including silicon-based mechanical devices, chemical and biological sensors and actuators, and miniature non-silicon structures (e.g. devices made from plastics or ceramics).

Overall applications areas of MEMS are in miniaturized devices in the automotive industry used for physical sensing and actuation; miniature sensors and instruments in medical and biotechnology applications based on chemical sensing; miniature devices in information technology (IT) and peripherals (including hard disk drive heads, micro-displays, and ink-jet print heads); optical steering in telecommunications and industrial automation [3-5]. Several fields and products have emerged over the years based on the applications of MEMS. BIOMEMS (which includes microfluidic structures, immunosensors, DNA arrays, etc.) deals with life-saving disposable diagnostic sensors, systems speeding up drug discovery, small pills for improving delivery, etc., most of these devices being disposable [6, 7]. Mechanical MEMS deals with micro-resonant sensors like accelerometers and gyroscopes. Optical MEMS or MOEMS involve micromirror arrays, fiber optic connectors, etc., whereas radio frequency MEMS (RFMEMS) involve inductors, capacitors, antennaes, etc. [8]. Commercial off-the-shelf microelectromechanical systems or COTS_MEMS, and high-aspect-ratio MEMS (HARMEMS) have also been introduced, and many more are expected [9, 10].

In this work, surface micromachining was used on silicon (Si) substrates or wafers to fabricate MEMS structures in a class 1000 clean room facility [11]. Phosphorous N-doped, single-side polished, 500µm thick Si wafers were used for the work. The material used in fabricating the vibrating structures was Gold (Au); chosen because of its good conductivity and reflective surfaces that eases optical resonance measurements [12]. A thin layer of Au deposited on top of Titanium (Ti) was also used to define the bottom actuating electrode [13]. There were six key processing techniques used in the fabrication. These were: plasma enhanced chemical vapour deposition (PECVD); optical lithography; vacuum evaporation [14]; electroplating [15]; dry release [16]; and wafer dicing [17]. The processing steps are shown in Fig. 3 and Fig. 4, and explained below in more details.

PECVD was used for the deposition of 0.5µm of silicon dioxide (SiO2) insulating layer using the Surface Technology Systems (STS) PECVD tool. In PECVD, a plasma is used to activate radicals, ions or highly excited species, which results in the deposited film whereas the ion bombardment of the substrate provides the energy required for them to settle as a stable film. Although it results into chemical particle contamination in form of hydrogen ions, PECVD is widely used because of its low substrate temperature, good adhesion, low pinhole density, as well as good coverage [18, 19]. PECVD is shown by letters A and C in Fig. 3.

Photolithography was used for optical patterning of the deposited layers before etching to form the required structures. This process was composed of photoresist spin coating, soft baking of the coated wafer to promote photoresist adhesion and release of any solvent, photomask alignment followed by ultraviolet exposure, and finally the photoresist develop. A positive photoresist was used that meant that the exposed areas of the pattern were removed by the developer [20, 21]. Photolithography is shown by letters D, F and H in Fig. 3.

Vacuum evaporation was used for the deposition of the thin film layers of Ti and Au inside a BOC Edwards Auto 500 evaporator. It is a form of physical vapour deposition (PVD) inside a low pressure PVD reactor in which the vaporised materials encounter few intermolecular collisions while travelling to the substrate in a line of sight format [22, 23]. Vacuum evaporation is shown by letters B and G in Fig. 3.

Electroplating was used for the electrodeposition of Au onto a dielectric silicon dioxide layer coated with a low resistance, thin adhesive film of Ti acting as a seed layer. Areas for electrodeposition are normally defined by a ultraviolet (UV) exposed pattern in a spin-coated polymer, which on developing away the exposed resist, establish contact with the

seed layer. This process was carried out in an electrolytic cell with the surface to be plated acting as the cathode in a plating

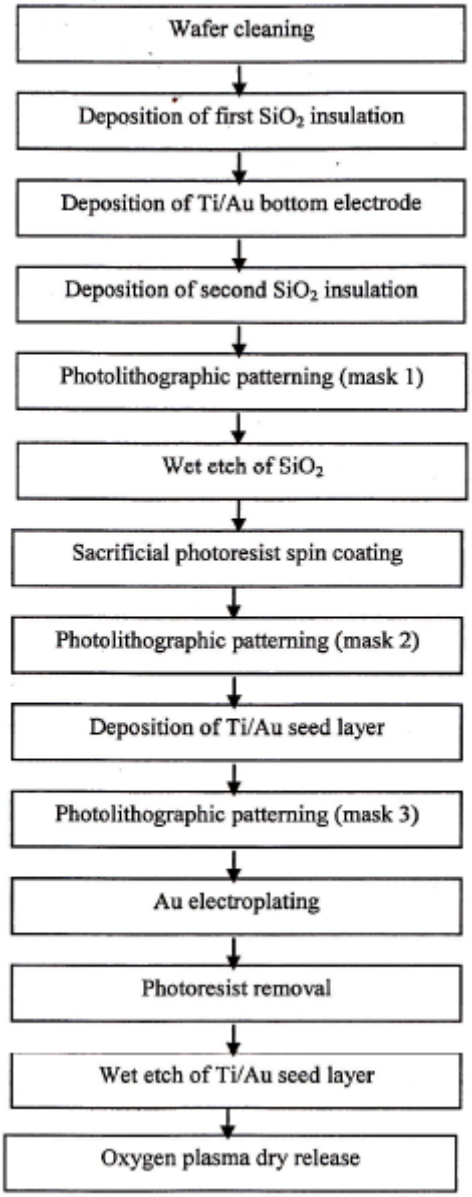

Fig. 4. Outline of the major manufacturing steps

solution made of the metal to be deposited, and the anode made of a material not readily attacked by the solution [24]. Electroplating is shown by letters I in Fig. 3.

Dry release was used as a stiction-free oxygen plasma stripping or ashing process of the photoresist layer which was acting as a sacrificial layer, resulting into a free hanging structure. Unlike wet stripping, dry release is controllable, causes no photoresist undercuts or broadening and leaves a less corrosive and cleaner surface [25]. Dry release is shown by letter L in Fig. 3.

Wafer dicing is the sawing process of the finished wafer into the individual dies or devices ready for packaging and testing. With the wafer mounted on a sticky tape onto the dicing saw machine, a saw blade consisting of a thick-shaped hub a diamond or carbide grit impregnated rim and rotating at several thousand revolutions per minute, encounters the wafer at a feed rate of the order of a centimeter per second to partially or completely cut through it [17].

II. METHODOLOGY

This design of experiments for the fabrication process was intended to solve the design challenges by careful arrangement of all steps in a sequence that is compatible to each other. The advantage of these fabrication process are its simplicity: the fact that it is released on the wafer level using surface micromachining as opposed to bulk micromachining; it employs only standard micromachining procedures like evaporation, photolithography, etc.; and it uses only three masks. The process steps followed in the fabrication of the prototype for the testing frequency tuning are outlined in Fig. 4. From this flow chart, the major steps are (i) deposition of initial SiO2 insulation, lower (Ti/Au) metal electrode, the second SiO2 insulation, and the sacrificial layer; (ii) vacuum evaporation of Ti/Au seed layer, electroplating of gold as the main structural material; (iii) release of the plated device. An illustration of the major steps is shown in Fig. 3. Some of the steps are explained further below:

A. Deposition of first insulating silicon dioxide layer

The fabrication of the two-terminal device began with 0.5µm of PECVD SiO2 onto the silicon wafer to insulate the Ti/Au from contact with the silicon substrate. The thickness of the PECVD SiO2 was measured using the Filmetrics F20 thin film measurement system. SiO2 thicknesses were measured from five different locations around four wafers and the overall average thickness of the deposited PECVD oxide was 5181±26Å.

B. Deposition of bottom Ti/Au metal electrode

In this work, the vacuum evaporation technique was employed to deposit thin electrically conductive metal films forming the bottom actuation electrode used in the electrostatic pull-down process and resultant frequency tuning. Titanium (Ti) metal, 30 nm thick was evaporated onto the insulating SiO2, followed by 100 nm of Gold (Au). Ti readily adheres to the surface of the oxide and to Au. Gold was chosen for its low resistivity, ease during both evaporation and wire bonding while packaging. The BOC Edwards Auto 500 evaporator was used to deposit the Ti/Au lower metal electrode.

C. Electroplating Process employed to deposit Au

In this work, the electroplating was used to deposit Au thickness of 2µm in a thiosulfate-sulfite bath and process started with the calculation of the plating area. This key parameter dictates the final thickness of the plated material. The exposed area for electroplating was 5.6 cm2. Using the atomic mass of Au of 196.67 g/mole, and a density of 19.3 g cm-3, an area of 5.6 cm2 with a plating current of 11 mA, would take approximately 20 minutes to deposit 2µm of Au.

D. *Dry Release*

The electroplated gold beam structures were released by completely etching away the photoresist sacrificial layer in an oxygen (O2) plasma asher using end-point detection and over etch technique. During the process, the flow rate of O2 was set at 800 ml/min, the chamber pressure at ~1mbar, and the microwave power at 500W.

E. *Wire Bonding*

In this work, a thin wire originating from a gold ball was used to connect both the top and bottom electrodes on the device to the pins on the chip package. This was done using the Kulicke and Sofa model 4124/8 Thermosonic Gold Ball Bonder. Because both electrodes are made of gold, it was easy to attach the gold ball during the bonding. Prior to wire bonding, the device was glued to the package using UHU plus End fest 300 Epoxy-based adhesive.

III. RESULTS AND DISCUSSION

The XL30 ESEM-FEG scanning electron microscope (SEM) was used to closely inspect the released devices, to measure the cantilever thickness as well as the separation gap between the cantilever and the insulated substrate with a resolution of 2nm [26].

This was done progressively as the release process was being optimized to obtain relatively flat cantilever beams. Initially, released beams were bent upwards due to residual stress as shown in Fig. 5. These devices were released with a plasma power of 500W after 12 minutes of oxygen ashing.

After lowering the oxygen plasma power to 250W, and the ashing release time to 7.5 minutes, flat beams were observed as shown in Fig. 6. To analyse the gap between the beams and the substrate, close-up views of the beam tips and sides were taken as shown in Fig. 7. Additionally, the thickness of the beam was measured as shown in Fig. 8. The Olympus MX 50T inspection microscope attached to a BRSL 'David' measurement system was used for visual inspection of the manufactured devices at various process steps for defects and to measure the dimensions with 0.5µm accuracy. The overall dimensions of the device are as shown in Table I. Line and width dimensional measurements of the shorter cantilever are shown in Fig. 9.

From the results shown in the preceding paragraphs, it is evident that initially, the released beams were not ideally flat. The end-tip was bent upwards with the initial deflection increasing with the length of the beam as shown in Fig. 5. This bending was attributed to several factors: firstly the high temperatures that are involved in the oxygen ashing process introduced thermal stresses. These temperatures depended on the oxygen plasma power and the duration of the ashing process. As the device was removed from the asher, the difference in temperature causes the beam tip to bend since the other end is fixed. Secondly, there could have been a deposition tensile stress due to the electroplating bath. This is because several wafers based on different processes were used in the same plating bath as this work. These wafers might have introduced impurities in the plating solution that resulted in a change in the stress of the deposited Au film. Other factors that could have resulted in a change in the stress include: the bath life and aging of the plating solution; plating without additives, accelerators and suppressors in the solution that should have increased plating throwing power and uniformity; and not annealing the device after plating. Additionally, the upward bending could also be attributed to the thermal mismatch between the thin Ti metal underneath the Au seed layer, and the electroplated Au.

On the whole, the deflection of the released cantilever beams was dependent on the dry-release ashing process time, and it was concluded that thermal stress was incurred during the plasma etching process. Since this additional stress can be inconclusively distinguished from the deposition stress, the post-deposition process such as a dry-release method also needs to be controlled for accurate characterization. Several solutions might be available including the use of a bridge (fixed-fixed) beam configuration to cancel the stresses. An immediate solution, which was employed in this work was to change the ashing process recipe to allow for low plasma power and intermittent ashing. Results show that an optimum ashing time can be reached where the beams are almost entirely flat. These are shown in Fig. 6 and Fig. 7. No stiction was observed in the cantilevers.

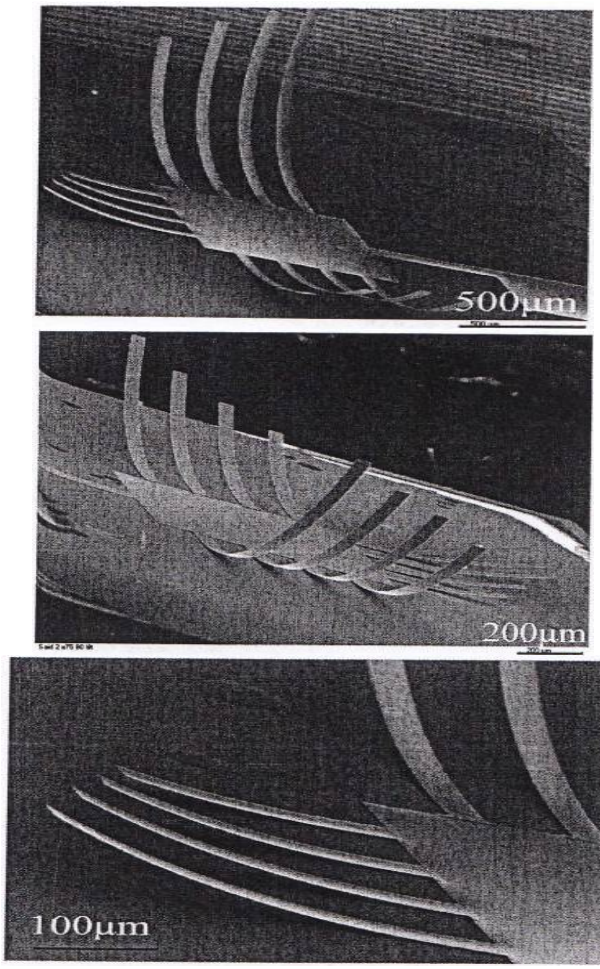

(a) *(b)* *(c)*

Fig. 5. SEM images of the suspended beams before the oxygen

plasma ashing power was optimised: (a) all beams wide view; (b) close up view of the longer beams (c) close-up view of the shorter beams

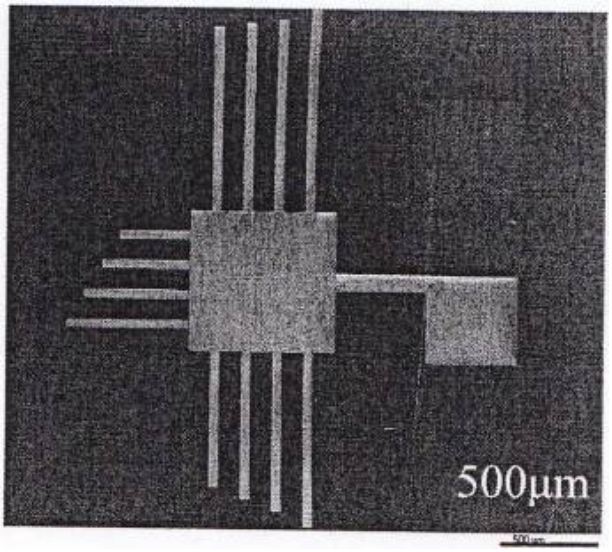

(a)

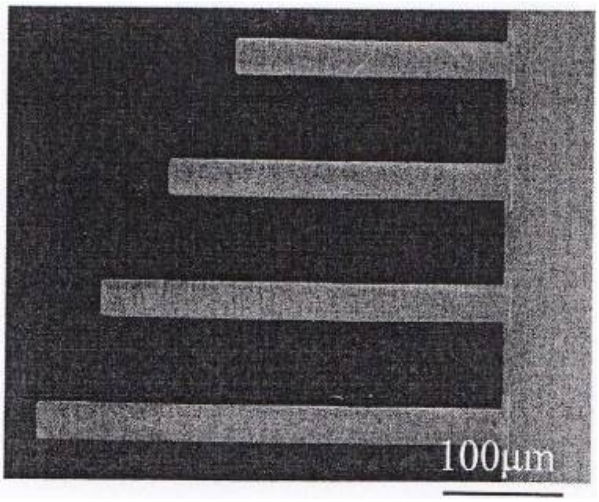

(b)

Fig. 6. SEM images of the flat beams after optimizing the plasma ashing process: (a) all beams wide view; (b) close-up view of the shorter beams

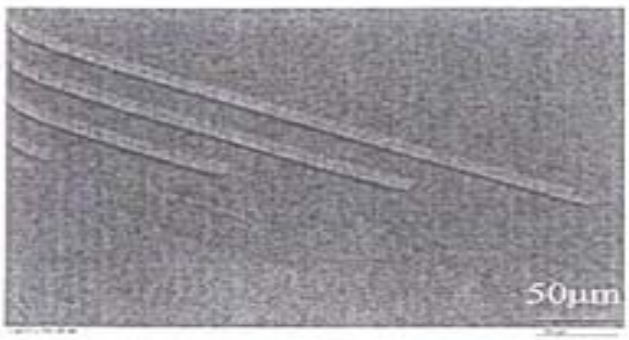

(a)

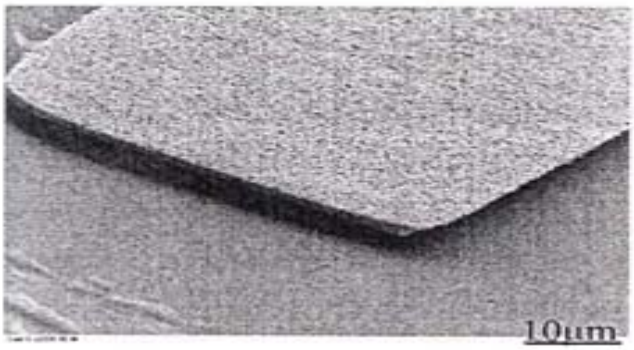

(b)

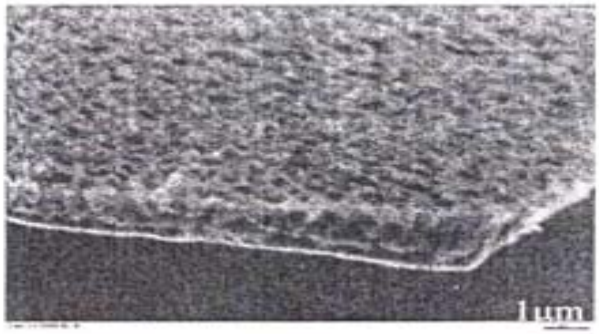

(c)

Fig. 7. SEM images of the flat beams after optimizing the plasma ashing process: (a) some of longer beams wide view; (b) close-up view of the beams (c) much closer view of the beam for thickness measurement

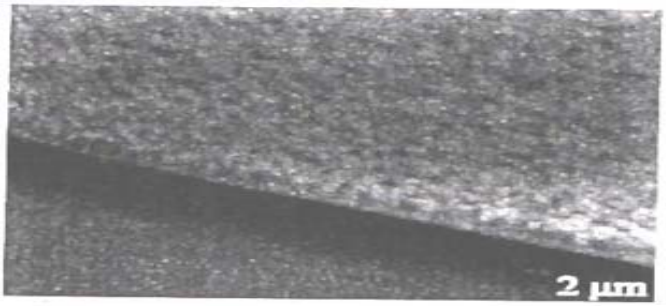

Fig. 8. SEM images much closer view for thickness of the beam measurement

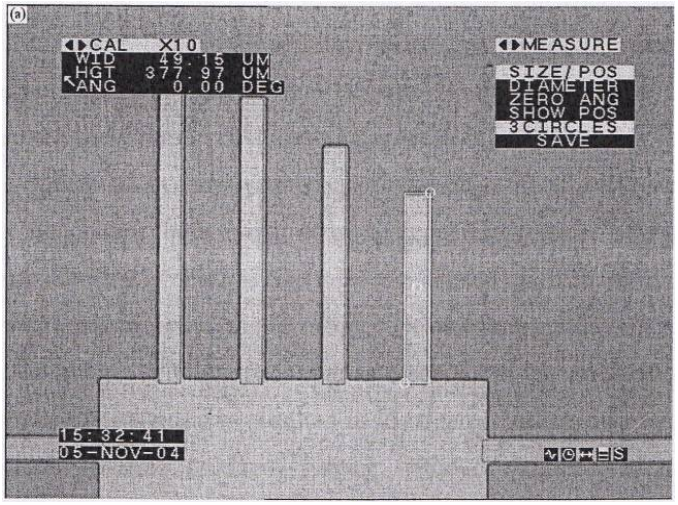

Fig. 9. Optical Microscope dimensional measurements for the shorter beams

TABLE I. RESULTS OF OPTICAL MEASUREMENTS OF THE BEAM DIMENSIONS

Device ID	Beam Length Lo±0.01 (µm)	Beam Width b±1.12 (µm)	Beam Thickness d±0.03 (µm)	Electrostatic gap H±0.63 (µm)
Beam 1	377.97	49.05	2.15	2.48
Beam 2	495.50	53.66	2.24	2.31
Beam 3	598.20	51.86	2.23	2.15
Beam 4	699.10	52.86	2.18	2.42
Beam 5	800.00	55.86	2.21	2.01
Beam 6	891.00	50.25	2.23	2.49
Beam 7	992.79	52.86	2.21	2.37
Beam 8	1090.09	49.86	2.25	2.16
Beam 9	1192.79	53.66	2.15	2.05
Beam 10	1290.09	50.45	2.22	2.30
Beam 11	1390.99	51.66	2.16	2.23
Beam 12	1491.89	52.66	2.14	2.48

SUMMARY

A fabrication process for the length tuning device has been described using controlled experiments. The process followed a surface micromachining procedure on a silicon wafer as a substrate. Standard lithography techniques were employed in the fabrication process and a set of three lithographic masks used to define the component layers of the cantilever device have been illustrated. The device after fabrication consisted of cantilever arrays that, together with the bottom electrode, form a vibrating microelecromechanical (MEMS) device. The fabrication recipe involved spin-coated resist as the sacrificial layer, which was dry etched using oxygen plasma ashing to release the cantilevers. The vibrating microstructure was made out of electroplated Au. By lowering the plasma power, and decreasing the ashing time, stresses induced during the release process were reduced thus avoiding stress-induced bending of the cantilever tips. The released cantilevers were relatively flat and stiction free with dimensions ranging from 377.97±0.01µm to 1491.89±0.01µm in beam length, 52.06±1.93µm beam width, 2.21±0.05µm beam thickness, and an electrostatic gap of 2.29±0.17µm above a 4934±3Å thick SiO2 insulation between the two electrodes. These values were in line with the designed device dimensions.

REFERENCES

[1]. Madou, M., 2002, Fundamentals of microfabrication: the science of miniaturization, pp. 615-666.

[2]. Petersen, K.E., 1982, Silicon as a mechanical material, Proceedings of the IEEE, 70(5), pp. 420-457.

[3]. Smith, C., et al., 1996, Monolithic integration of waveguide structures with surface-micromachined polysilicon actuators, Proc. SPIE, 2722, pp. 75-81.

[4]. Guckel, H., 1991, Surface micromachined pressure transducers, Sensors and Actuators, A(28), pp. 133-146.

[5]. Krebs, G. A., 1993, A low power integrated catalytic gas sensor, Sensors and Actuators, B13-14, pp. 155-158.

[6]. Li, C., et al, 2002, Progresses in BioMEMS and biochip technologies, Zhongguo Jixie Gongcheng/China Mechanical Engineering, 13(1), pp. 39.

[7]. Shawgo, R. S., et al, 2002, BIOMEMS for drug delivery, Current Opinion in Solid State and Materials Science, 6(4), pp. 329-334.

[8]. De Luis, J.R., et al, 2010, A tunable asymmetric notch filter using RFMEMS, Microwave Symposium Digest (MTT), 2010 IEEE MTT-S International, pp.1146-1149.

[9]. Holbert, K.E. et al, 2010, Performance of Commercial Off-the-Shelf Microelectromechanical Systems Sensors in a Pulsed Reactor Environment, IEEE Radiation Effects Data Workshop (REDW), pp. 8.

[10]. Hutchison, D.N., et al, 2010, Carbon Nanotubes as a Framework for High-Aspect-Ratio MEMS Fabrication, Journal of Microelectromechanical Systems, 19(1), pp. 75-82.

[11]. Kim, J., et al, 2001, Why is (111) silicon a better mechanical material for MEMS, Proc. Transducers 2001, pp.662 -665.

[12]. Villain, J., et al, 2008, Determination of Mechanical Properties of Electronic Materials as Gold, Nickel and Tin using Nanoindentation, EPTC 2008. 10th Electronics Packaging Technology Conference, pp. 304-309.

[13]. Winter, M., 1993-2012, WebElements: the periodic table of the elements gold titanium essential information, http://www.webelements.com/gold/, The University of Sheffield and WebElements Ltd, UK, 11/4/2012.

[14]. Klenk, R., et al, 1993, A model for the successful growth of polycrystalline films of CuInSe2 by multisource physical vacuum evaporation, Advanced Materials, 5(2), pp. 114-119.

[15]. Angurel, L.A. et al, 2007, Electrodeposition of Silver Gold Alloys on Bi2Sr2CaCu2O8+d Ceramics, IEEE Transactions on Applied Superconductivity, 17(2), pp. 3012-3015.

[16]. Keller, S. et al, 2007, Optimized plasma-deposited fluorocarbon coating for dry release and passivation of thin SU-8 cantilevers, Journal of Vacuum Science & Technology B: Microelectronics and Nanometer Structures, 25(6), pp. 1903-1908.

[17]. Lee, H., et al, 2007, Method for dicing semiconductor wafers, Patent number: 7183137, Application number: 10/725, pp. 697.

[18]. Bhal Singh, C. et al, 2011, Raman spectroscopy study of growth of multiwalled carbon nano-tubes using Plasma Enhanced Chemical Vapour Deposition, International Conference on Nanoscience, Engineering and Technology (ICONSET), pp. 252-257.

[19]. Roszairi, H. and Rahman, S.A., 2002, High deposition rate thin film hydrogenated amorphous silicon prepared by d.c. plasma enhanced chemical vapour deposition of helium diluted silane, Proceedings ICSE 2002, IEEE International Conference on Semiconductor Electronics, pp. 300-303.

[20]. Sun, Y., et al, 2011, Room-Temperature Operation of Silicon Single-Electron Transistor Fabricated Using Optical Lithography, IEEE Transactions on Nanotechnology, 10(1), pp. 96-98.

[21]. Wong, A. K., 2001, Resolution enhancement techniques in optical lithography, SPIE Press, pp. 214.

[22]. Yeganeh, M. and Torabi, Z., 2011, Characterisation of copper thin film oxidation deposited by electron beam physical vapour deposition at low temperatures, IET Micro & Nano Letters, 6(11), pp. 884-887.

[23]. Miranda, D.O. et al, 2010, mc-Si thin films by hydrogen plasma assisted vacuum evaporation, 35th IEEE Photovoltaic Specialists Conference (PVSC), pp. 003706-003708.

[24]. Parthasaradhy, N. V., 1989, Practical Electroplating Handbook, Prentice-Hall, Inc. (USA), pp. 1444.

[25]. Shuzo, F., et al, 1991, Resist stripping in an O2+H2O plasma downstream, Journal of Vacuum Science & Technology B: Microelectronics and Nanometer Structures, 9(2), pp. 357-361.

[26]. Griffin, N. S., 1994, Enhanced topography imaging in the scanning electron microscope, Measured Science & Technology, 5(11), pp.1403-1406.

BIOGRAPHY

Said Kafumbe is currently a Faculty at the Higher Colleges of Technonoly – Abu Dhabi Womens College. Dr. Kafumbe holds a Bachelor of Science degree in Electronics and Telecommunications Engineering from the University of Dar-Es-Salaam in Tanzania, a Master of Science degree in Electrical and Electronics Engineering from the Middle East Technical Uinveristy in Turkey, and a Ph.D in Electrical and Electronics Engineering from Newcastle University in UK. He has over 16 years of experience working both in the telecoms and semiconductor manufacturing industries as well as in academia and is a member of IEEE and an associate member of IEE. He has published several journal papers and his research interests range from MEMS, Nanotechnology, Embedded wireless sensor system, as well as in renewable energy harvesting.

Ravichandran. Danthakani is currently working as academic faculty/ instructor at higher colleges of Technology (HCT), Abu Dhabi. Mr. Ravichandran holds a Bachelor of Engineering in Electronics and Communication Engineering from Madras University and Master of Engineering in Electronics and Communication Engineering specialization Medical Electronics from Anna University. He has approximately 20 years of experience out of which 14years had been in academics and 6 years in various electronics industries. He is teaching various electronics, communication, control and microelectronic courses. His experience in manufacturing industry had been programming various mechatronic machines for electronics industry, testing and maintenance. Mr. Ravichandran is an active member of academic development committee at HCT and he served as member of Development Committee at various universities he worked for. Mr. Ravichandran is a member of Institution of Engineers, Institute of Electronics and Telecommunication Engineering and Chartered Engineer by profession.

Emad Abd-Elrady received the B.Sc. and M.Sc. degrees in ElectricalEngineering from Ain Shams University, Cairo, Egypt in 1993 and 1997, respectively. He received the Licentiate and Ph.D. degrees in Electrical Engineering with specialization in Signal Processing from Uppsala University, Sweden in 2002 and 2005, respectively. From January 2006 to March 2009, he was a senior researcher at Christian Doppler Laboratory for Nonlinear Signal Processing, Graz University of Technology, Austria. From March 2010 to January 2011, he was a research fellow at Institute for Digital Communications, The University of Edinburgh, Scotland, UK. Since February 2011, he has been electronics engineering faculty at Abu Dhabi Women's College, United Arab Emirates.

Mohamamd. Alqudah is currently working as academic faculty/ instructor at higher colleges of Technology (HCT), Abu Dhabi. Mr. Alqudah holds a Bachelor of Engineering in Electronics and Communication Engineering from Yarmouk University in Jordan and Master of Engineering in Electronics and Communication Engineering specialization Digital Communication from Middle East Technical University in Turkey. He has approximately 25 years of experience out of which 17 years had been in academics and 8 years in IT field. He is teaching various electronics, communication, control, computer and Mathematics courses. His experience in teaching, setting up computer networks and in building database school management applications. Mr. Alqudah is an active member of Jordan Engineers Association.